ISSN 0010-9525, Cosmic Research, 2024, Vol. 62, No. 2, pp. 187–196. © Pleiades Publishing, Ltd., 2024.

Earth's Ionospheric Response to Solar Activity Phenomena in February–March 2023

F. I. Vybornov[a, b, *] and O. A. Sheiner[a, **]

[a] *Lobachevsky State University of Nizhny Novgorod, Nizhny Novgorod, 603950 Russia*

[b] *Volga State University of Water Transport, Nizhny Novgorod, 604005 Russia*

**e-mail: vybornov@nirfi.unn.ru*

***e-mail: rfj@nirfi.unn.ru*

Received August 15, 2023; revised October 9, 2023; accepted October 17, 2023

Abstract—As a result of the analysis of data from vertical and oblique sounding of the ionosphere in February–March 2023 using the new ionospheric index, it was found that solar coronal mass ejections (CMEs) of the loop type lead to a long-term decrease in the critical frequencies *F*-layer of the ionosphere, while other types of CMEs may not lead to significant changes in the state ionosphere. The possible role of high-speed streams of solar wind and energetic protons in the occurrence of ionospheric disturbances is noted. Distance–frequency characteristics of the Cyprus–Nizhny Novgorod route during geomagnetic disturbances are given, which indicate both a strong deformation of the *F*-layer of the ionosphere and the appearance of *z*-shaped wave disturbances propagating to a region of lower altitudes.

DOI: 10.1134/S0010952523600294

INTRODUCTION

In recent years, much attention has been paid to the causes of ionospheric disturbances and the dynamics of their development. This is due to the widespread use of long-distance short-wave radio communications and over-the-horizon radar, as well as the need to improve the reliability of their operation and the predictability of the parameters of the ionospheric communication channel [1–3]. The state of the ionosphere affects the operation of satellite radio navigation systems and can limit the positioning accuracy of ground objects [4–6].

The emergence of a large number of research satellites and ground-based diagnostic tools for space weather parameters makes it possible to obtain a huge amount of data, where the ionosphere can already act as a medium that is a sensitive indicator of solar–terrestrial connections.

According to numerous previous studies (see, for example, [7–14]), ionospheric parameters are strongly dependent on geoeffective phenomena occurring on the Sun, such as coronal mass ejections (CMEs) and high-speed solar wind streams (HSSs). Registration of disturbances in the ionosphere can be carried out both by ground-based sensing means (vertical, oblique and back-tilt sounding ionosondes, riometers, incoherent scatter radars, etc.) and by using rockets and artificial Earth satellites (direct measurements, the use of onboard ionosondes or the use of transionospheric sounding methods using satellite signals) [15].

This article examines the influence of solar geoeffective disturbances on the ionospheric parameters in February and March 2023. As ionospheric parameters, variation in the time of critical frequency f_0 of the F_2-layer of the ionosphere during vertical sounding (VS) and the maximum observed frequency (MOF) during oblique sounding (OS) of the ionosphere were studied using the method of a linear frequency modulated (chirp) signal using the new ionospheric index that we proposed earlier [16].

DATA AND METHODS

The study used data from vertical and oblique sounding of the ionosphere. Critical frequency values of the *F*-layers of the ionosphere are given according to data (https://ulcar.uml.edu/stationlist.html, https://wdc.kugi.kyoto-u.ac.jp/igrf/gggm/index.html) of the Tromsø (69.6° N, 19.2° E, geographical coordinates; 36.26° N, 103.07° E, geomagnetic coordinates), Warsaw (52.21° N, 21.06° E; 50.48° N, 105.18° E), and Athens (38.0° N, 23.5° E; 36.26° N, 103.07° E) ionospheric stations. The choice of these stations was determined by their close location to one meridian, which makes it possible to estimate the rate of development of ionospheric disturbances from the polar oval to the equator.

Critical frequencies of the *F*-layer of the ionosphere were obtained according to data from the CADI ionosonde located in Vasilsursk (56.15° N,

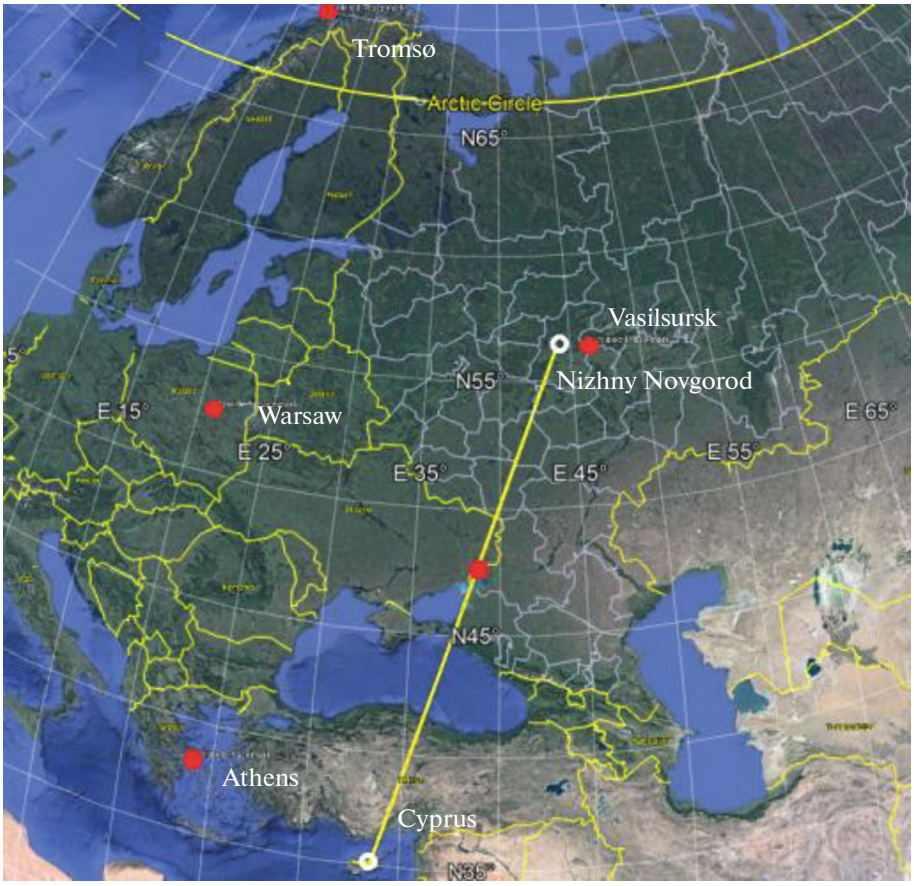

Fig. 1. Relative positions of vertical (marked with red dots) and oblique sounding stations (yellow line). The midpoint of the Cyprus–Nizhny Novgorod route is marked with a red dot.

46.10° E; 50.77° N, 129.13° E) during special measurements. The ionosonde operated in a 15-min ionospheric sounding mode in the frequency range from 1 to 12 MHz. The maximum observed frequencies of the *F*-layers of the ionosphere are given based on the results of special measurements on the Cyprus–Nizhny Novgorod route. The chirp signal was received every 5 min in the range of 8–33 MHz. The coordinates of all VS stations, the data of which were used in the article, are given next to their names, and the relative positions of the VS stations (marked with red dots) and the oblique sounding routes (shown with a yellow line) are shown in Fig. 1. The midpoint of the Cyprus–Nizhny Novgorod route (also marked in this figure with a red dot) has coordinates 45.6° N, 37.45° E (geographic) and 41.61° N, 118.15° E (geomagnetic).

The new ionospheric index used in this study is based on calculating the deviation of the current value of critical frequency Δf_0 (or MOF) of the F_2 ionospheric layer from the average daily profile for a month, measured using the method of vertical (or oblique) sounding of the ionosphere [16]. Deviation Δf_0 at each moment of registration of the ionogram (for VS) or distance–frequency characteristic (DFC) of OS was determined as

$$\Delta f_{0jk} = f_{0jk} - \overline{f_{0j}},$$

where

$$\overline{f_{0j}} = \sum_{k=1}^{N} f_{0jk}/N,$$

f_{0jk} is the measured value, j is the number of the measurement point during the day, k is the number of days in a month, and N is the amount of days in a month. A similar procedure could be carried out when analyzing MOF oblique sounding data.

Fig. 2. Behavior of index $\Delta f_0 F_2$ for three ionospheric stations: (a) Athens, (b) Warsaw, (c) Tromsø; (d) time course of X-ray radiation and proton flux; indices (e) Kp and (f) *Dst*; graph of the speed of high-speed solar wind flows (V_{HSS}, km/s) for February 2023. The horizontal axis is the days of the month; left vertical axis: for $\Delta f_0 F_2$, time of day (hour, UT); for all others, values of quantities.

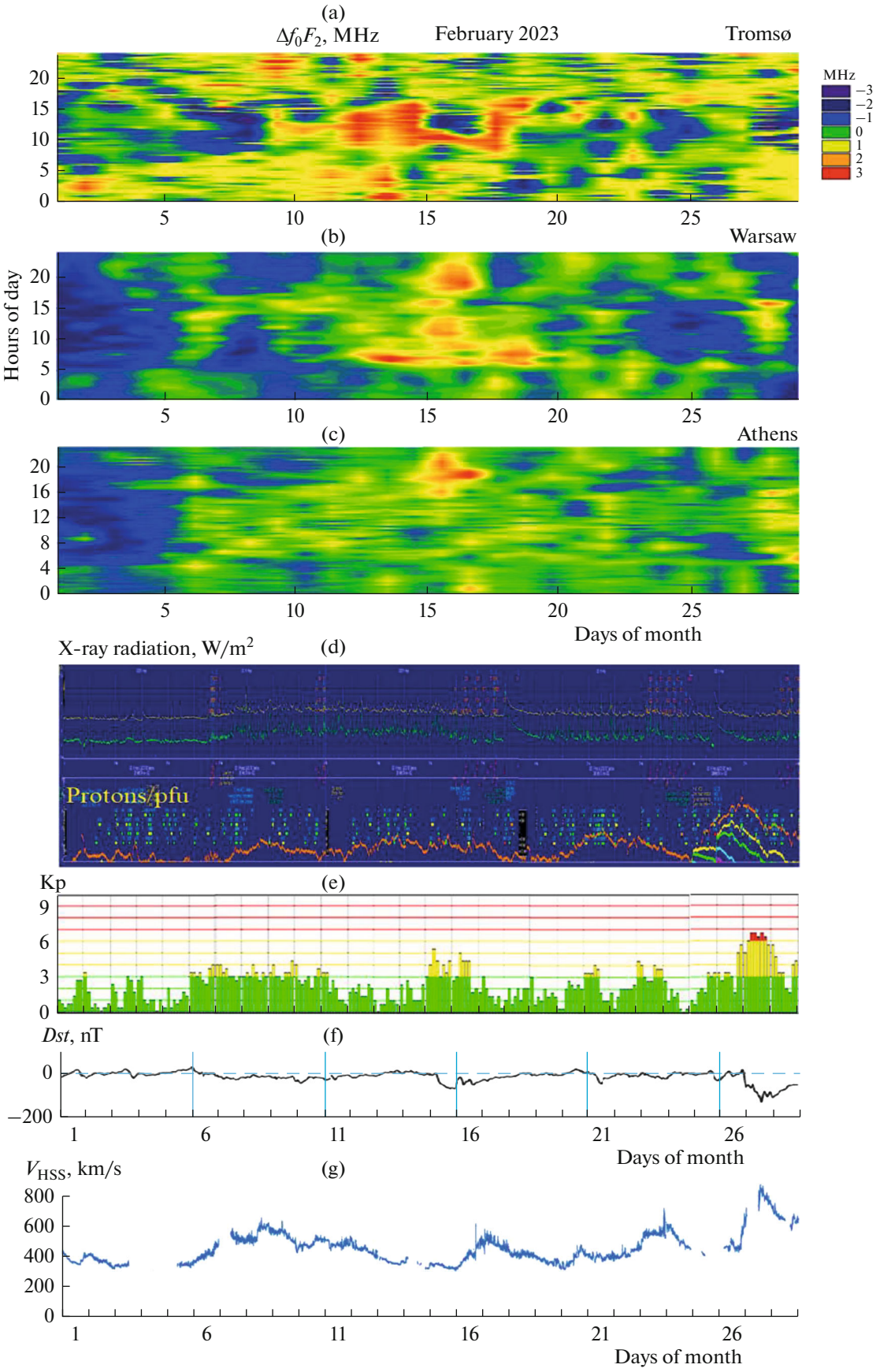
(a)
Δf_0F_2, MHz
February 2023
Tromsø
MHz
−3
−2
−1
0
1
2
3
(b)
Warsaw
Hours of day
(c)
Athens
Days of month
X-ray radiation, W/m^2
(d)
Protons/pfu
Kp
(e)
Dst, nT
(f)
Days of month
V_{HSS}, km/s
(g)
Days of month

The differential parameter we proposed for studying data from vertical and oblique sounding of the ionosphere allows us to eliminate stationary dependences (excluding the average daily behavior of f_0F_2 or MOF), and the color scheme used allows us to increase the sensitivity of detection of deviation Δf_0 depending on the time of day and day of the month.

Additionally, an analysis was carried out of the influence of increased geomagnetic activity on the mid-latitude ionosphere. For this purpose, a comparison was made of the Kp- and *Dst*-indices for February and March 2023 and ionograms of the Vasilsursk ionospheric station or DFC of the ionosphere for the Cyprus–Nizhny Novgorod route.

As events affecting the state of the Earth's ionosphere, coronal mass ejections of various types were primarily considered, including off-limb events recorded on the Sun in February–March 2023, as well as (if necessary) change in the speed of high-speed solar wind flows, fluxes of solar protons of different energies, and the dynamics of changes in short-wave (X-ray) radiation. Information on registration of coronal mass ejections is available in the CACTus Catalog (http://sidc.be/cactus). CME data are cataloged automatically using LASCO C2/C3 observations. Updated data on registration of coronal mass ejections are provided in the SOHO LASCO CME Catalog (https://cdaw.gsfc.nasa.gov/CME_list/).

Below in the text, dates, and times are given in Greenwich Mean Time in the form accepted for the journal, but the date and time on the images used for analysis are left in the form in which they are given on the source data sites.

For ease of comparison of data on deviation Δf_0 depending on the time of day and day of the month and coronal mass ejections central part of Figs. 2 and 3 (for the Warsaw station) is repeated with indication of the zones of influence of specific CMEs.

RESULTS

Examples of emerging ionospheric disturbances for observations carried out in February and March 2023 at three stations—Athens, Warsaw, and Tromsø—are shown in Figs. 2 and 3, respectively. Data are also given there on the indices Kp-, X-ray, and *Dst*, which indicate increased geomagnetic activity (https://tesis.xras.ru/magnetic_storms.html, https://wdc.kugi.kyoto-u.ac.jp/dst_realtime/202210/index.html)—at the end of both February and March, strong magnetic storms occurred—as well as and the time course of the speed of high-speed solar wind flows (V_{HSS}, km/s) (https://omniweb.gsfc.nasa.gov).

FEBRUARY 2023

Examples of comparisons between recorded CMEs and observed ionospheric disturbances in February 2023 are shown in Fig. 4 using the example of ionospheric data from Warsaw. Taking into account the Kp- and *Dst* indices, such a comparison allows us to identify a possible source of influence on the critical frequencies of the *F*-layer of the ionosphere and consider a CME as a source of ionospheric disturbances.

Examples of coronal ejections in Figs. 4 and 7 are shown as difference images of the solar corona obtained in white light using the LASCO/C2 coronagraph. The boundaries of registered CMEs are marked in white in the image. Coronal mass ejections are visible as bright reflections.

The decrease in critical frequencies (clearly visible from the Warsaw station data) over the first ten days of February was associated with loop-shaped coronal mass ejections (CME) on February 3, 2023, at 10.00 UT; February 9, 2023, at 06.12 UT; and February 10, 2023, at 09.24 UT that were recorded by LASCO-C2 (http://sidc.be/cactus).

The increase in critical frequencies in the middle of the month was caused by radial emissions of CME on February 11, 2023, at 04.24 UT; February 12, 2023, at 17.00 UT; and February 15, 2023, at 00.24 UT, which were also recorded by LASCO-C2 (http://sidc.be/cactus).

The repeated decrease in critical frequencies according to the Warsaw station data at the end of the month (February 24–25) was associated with coronal mass ejections of the Halo type on January 24, 2023, at 20.36 UT and on January 25, 2023, at 19.24 UT (https://cdaw.gsfc.nasa.gov/CME_list/).

An increase in the speed of HSSs of the solar wind from 400 to 800 km/s on February 26 (https://omniweb.gsfc.nasa.gov) and coronal mass ejections on January 24, 2023, at 20.36 UT and on January 25, 2023, at 19.24 UT (https://cdaw.gsfc.nasa.gov/CME_list/) led to a strong magnetic storm, which began in the evening of February 26, 2023, and continued on February 27, 2023. At the same time, the critical frequencies changed sharply in the *F*-layer of the ionosphere. According to updated catalog data (https://cdaw.gsfc.nasa.gov/CME_list/), this may have been a response to coronal ejections on February 27, 2023, recorded on C2 at 01.48 and 10.24 UT.

The magnetic storm of February 27, 2023, had a significant impact on the mid-latitude ionosphere of the central region of Russia. According to the VS Vasilsursk station data, strong disturbances of critical frequencies and diffuse reflections were observed (*F*-spread), as well as the presence of multiple reflections. Figure 5

Fig. 3. Behavior of index Δf_0F_2 for three ionospheric stations: (a) Athens, (b) Warsaw, (c) Tromsø; (d) time course of X-ray radiation and proton flux; indices (e) Kp and (f) *Dst*; graph of the speed of high-speed solar wind flows (V_{HSS}, km/s) for March 2023. The horizontal axis is the days of the month; left vertical axis: for Δf_0F_2, time of day (hour, UT); for all others, values of quantities.

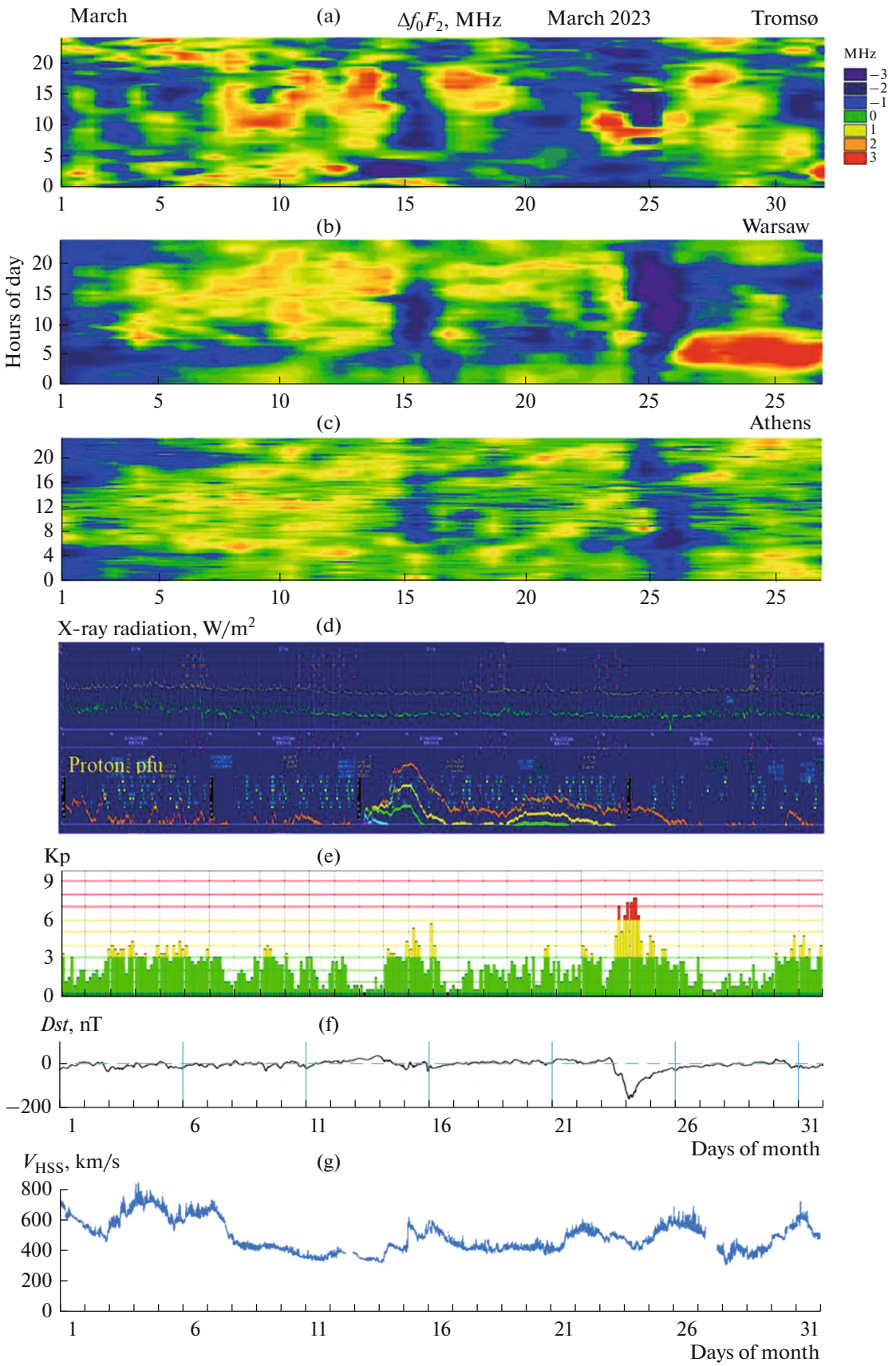
March
(a)
Δf_0F_2, MHz
March 2023
Tromsø
MHz
−3
−2
−1
0
1
2
3
Hours of day
(b)
Warsaw
(c)
Athens
X-ray radiation, W/m^2
(d)
Proton, pfu
Kp
(e)
Dst, nT
(f)
Days of month
V_{HSS}, km/s
(g)
Days of month

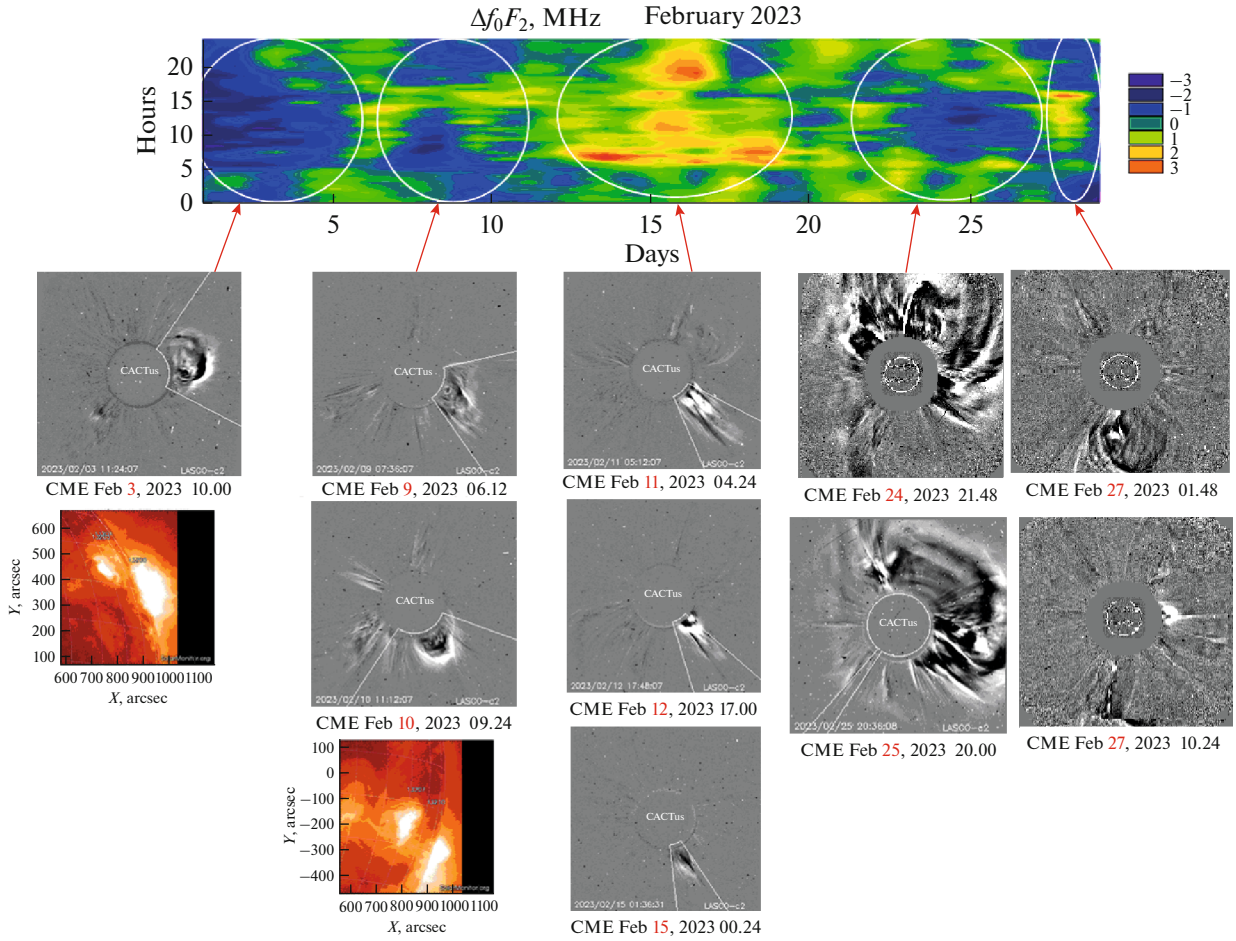

Fig. 4. Illustration of joint analysis of the behavior of index Δf_0F_2 for data from the Warsaw ionospheric station and CME registration in February 2023.

shows ionograms in which, at 12.00 UT (see Fig. 5a), a profile of the undisturbed ionosphere with a critical frequency was observed in the *F*-layer about 9.5 MHz. A sharp change in the appearance of the ionograms began at 12.45 UT. At 13.30 UT (see Fig. 5b), the critical frequency of the *F*-layer of the ionosphere decreased to 6 MHz, strong diffuseness was observed (up to three points). Subsequently, the critical frequency continued to decrease the *F*-layer of the ionosphere, stratification was observed in the region of critical frequencies (see Figs. 5c–5e), the reflected signal from the *E*- and F_1-layers stopped registering. Only at 6.00 UT on February 28, 2023, was the ionosphere completely restored. It should be noted that on the night from February 26 to 27, 2023, very strong diffuseness was observed in the *F*-layer of the ionosphere.

A magnetic storm also appeared on the Cyprus–Nizhny Novgorod chirp sounding route. On the distance–frequency characteristic of the chirp signal, *z*-shaped disturbances (a consequence of moving ionospheric disturbances, see Figs. 6a–6d, 6f), diffuseness, a strong *Es*-layer (see Figs. 6e, 6f). Severe distortion of the reflection tracks was observed. Not only the one-hop tracks, but also the two- and three-hop tracks, turned out to be distorted on the DFC. Strong back-slant scattering was observed.

MARCH 2023

In Fig. 7, graphs are provided Δf_0F_2 for March 2023 for data from the Warsaw station, which, taking into account Kp- and *Dst*-indices, allow one to identify a possible source of influence on critical frequencies of the *F*-layer of the ionosphere.

The decrease in critical frequencies at the beginning of the month may be a consequence of solar activity at the end of February, and at the same time a response to the CME on March 1, 2023. The long-term decrease in critical frequencies on March 2–10, 2023, may be a response to the CME on March 3–6, 2023, from the AR on the western limb.

The peculiarity of the ionospheric disturbances that occurred on March 13–17, 2023, is that they coin-

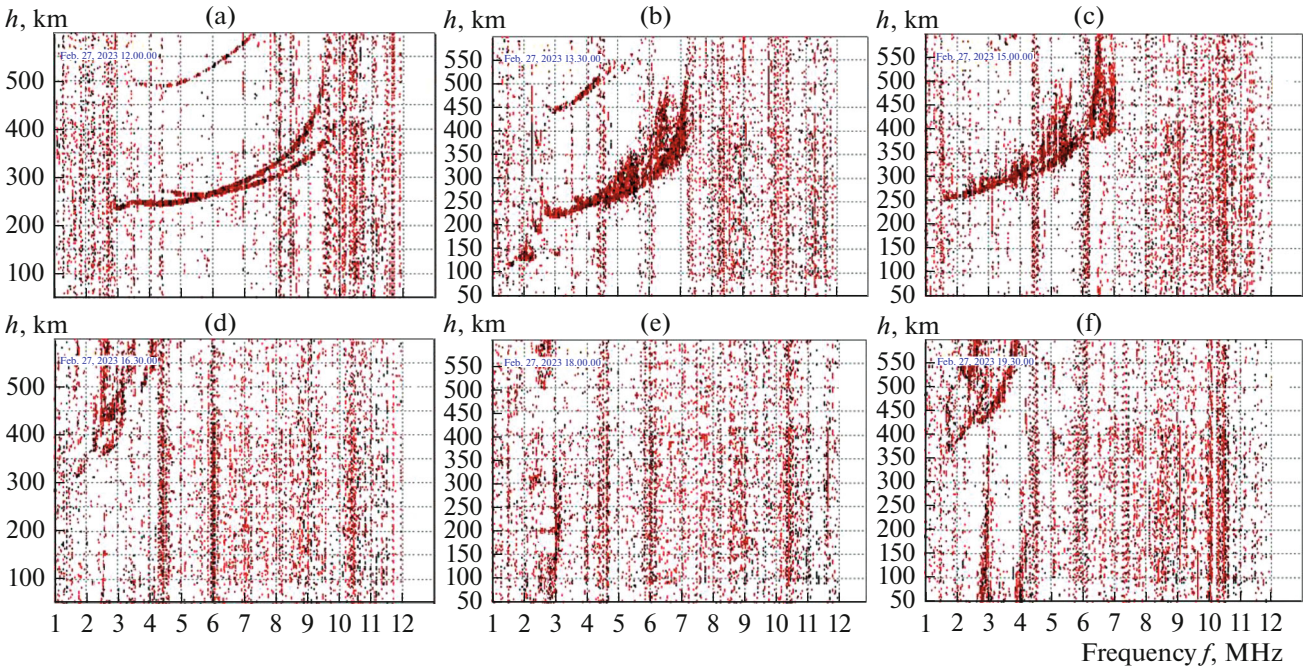

Fig. 5. Vertical sounding ionograms obtained at the Vasilsursk ionospheric station on February 27, 2023 ((a) 12.00, (b) 13.30, (c) 15.00, (d) 16.30, (e) 18.00, (f) 19.30 UT).

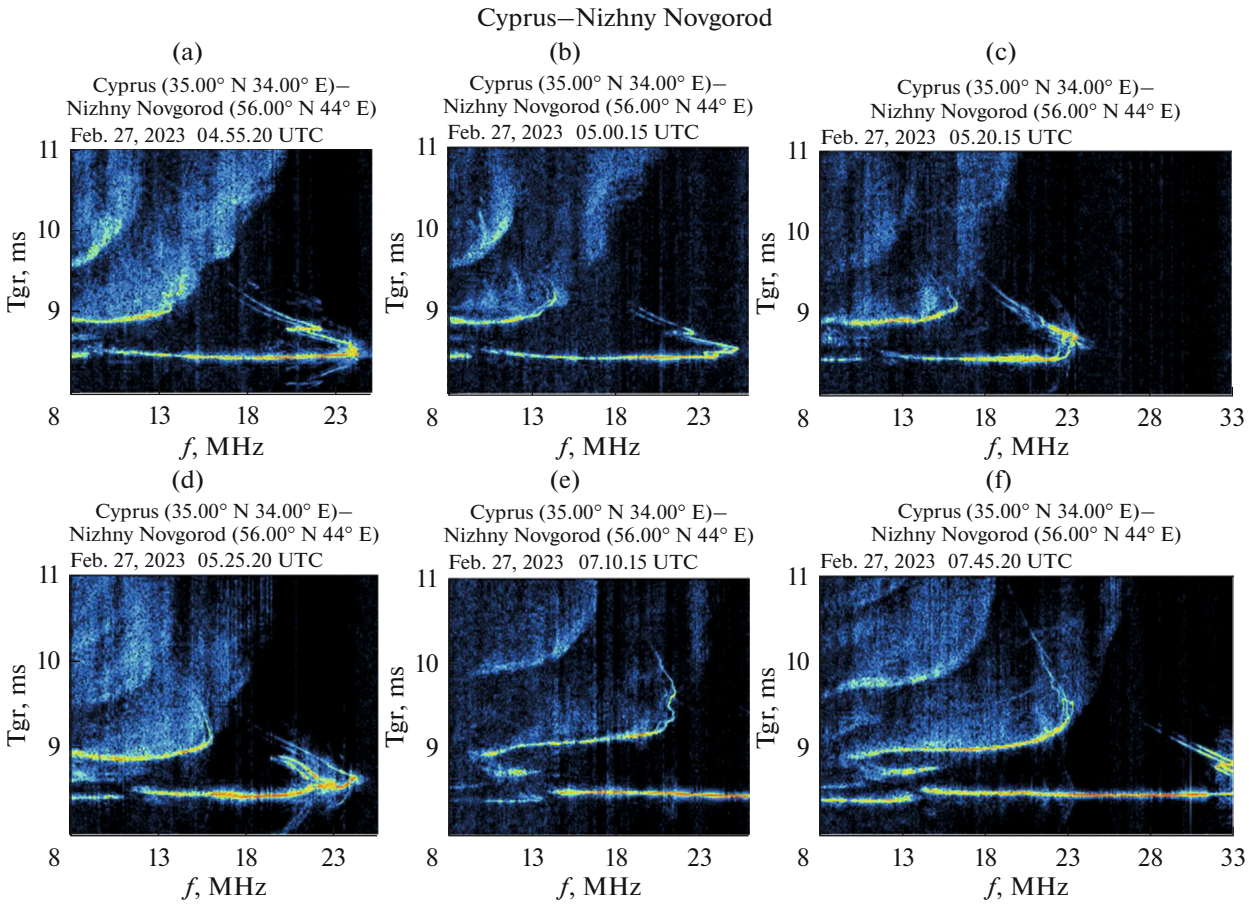

Fig. 6. Distance–frequency characteristic of the chirp signal along the Cyprus–Nizhny Novgorod sounding route on February 27, 2023 ((a) 04.55, (b) 05.00, (c) 05.20, (d) 12.00, (e) 05.25, (f) 07.10, (g) 07.45 UT).

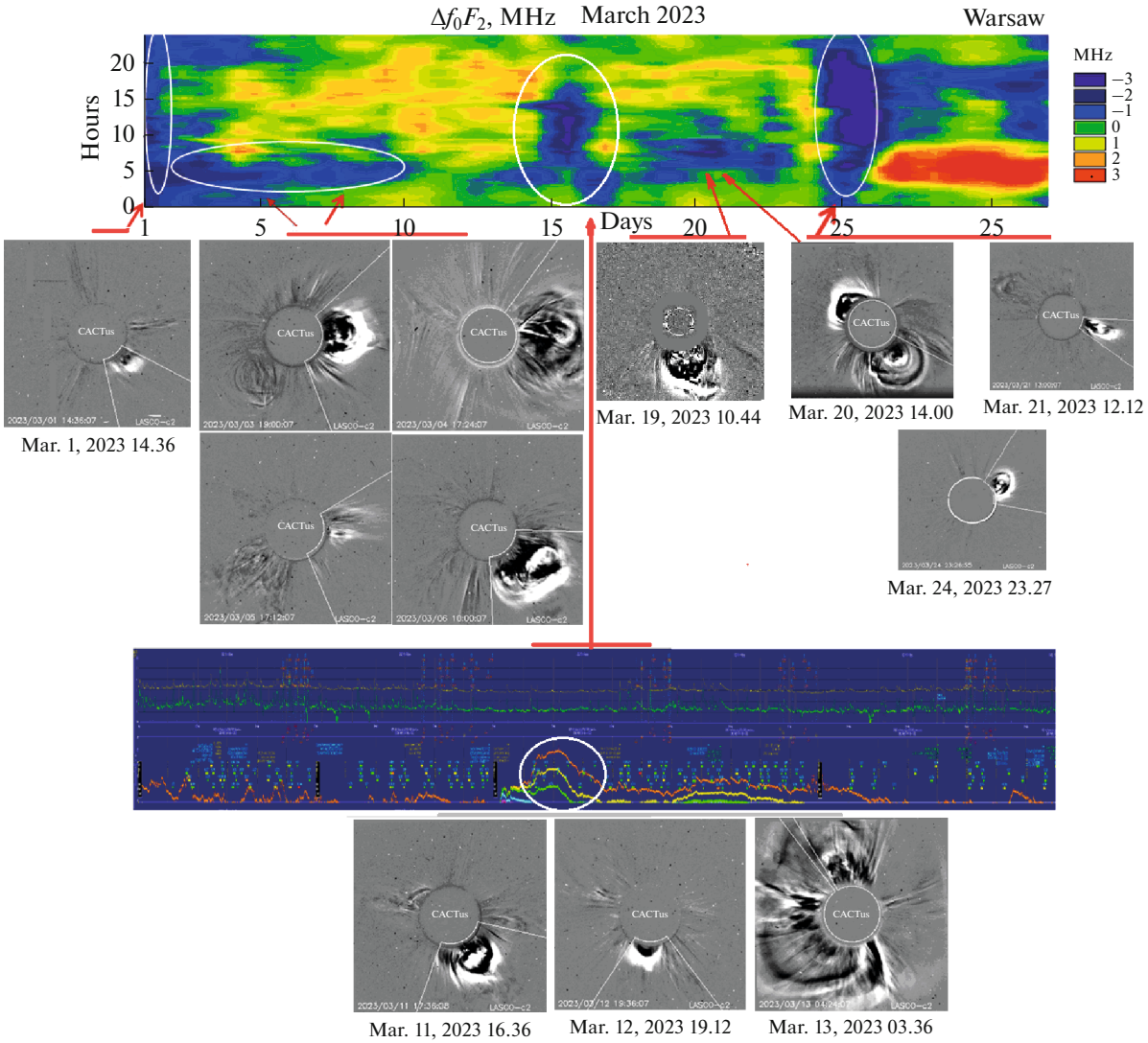

Fig. 7. Illustration of joint analysis of the behavior of index Δf_0F_2 for data from the Warsaw ionospheric station and CME registration in March 2023.

cide with a coronal mass ejection of very high power registered on March 13–17, 2023, on the side of the Sun farther from the Earth, which also became the source of the flow of solar protons. This is confirmed by the absence of a solar flare, with which the beginning of the event can be associated. An additional contribution to ionospheric disturbances can be made by Halo type CMEs on March 11–12, 2023 (https://cdaw.gsfc.nasa.gov/CME_list/).

Short-term disturbances of the ionosphere on March 20–21 are most likely associated with the response to the CME on March 19, 2023 and beyond the limb on March 20, 2023 (https://cdaw.gsfc.nasa.gov/CME_list/).

Disturbances in the ionosphere on March 24–25, 2023, are caused by coronal mass ejections on the opposite side of the Sun from the Earth; no solar flares were recorded during this period. The response is observed with a large delay, since the CME comes from behind the limb (March 20, 2023; Halo type, https://cdaw.gsfc.nasa.gov/CME_list/). At the same time, the CME of March 21–24, 2023 (https://cdaw.gsfc.nasa.gov/CME_list/), can make an additional contribution to the ionospheric response.

Figures 8a–8d show the distance–frequency characteristics of the chirp signal on the Cyprus–Nizhny Novgorod chirp sounding route obtained on March 23, 2023 ((a) 12.45, (b) 15.40 UT, (c) 17.10, and (d) 18.10 UT). Distance–frequency characteristics obtained at 15.40 and 17.10 indicate strong disturbance of the ionosphere. There are strong distortions in the shape of the tracks of one- and two-hop tracks. *z*-Shaped disturbances are clearly present (see Figs. 8b–8c). DFCs obtained at 12.45 and 18.10 UT indicate the absence of strong disturbances in the ion-

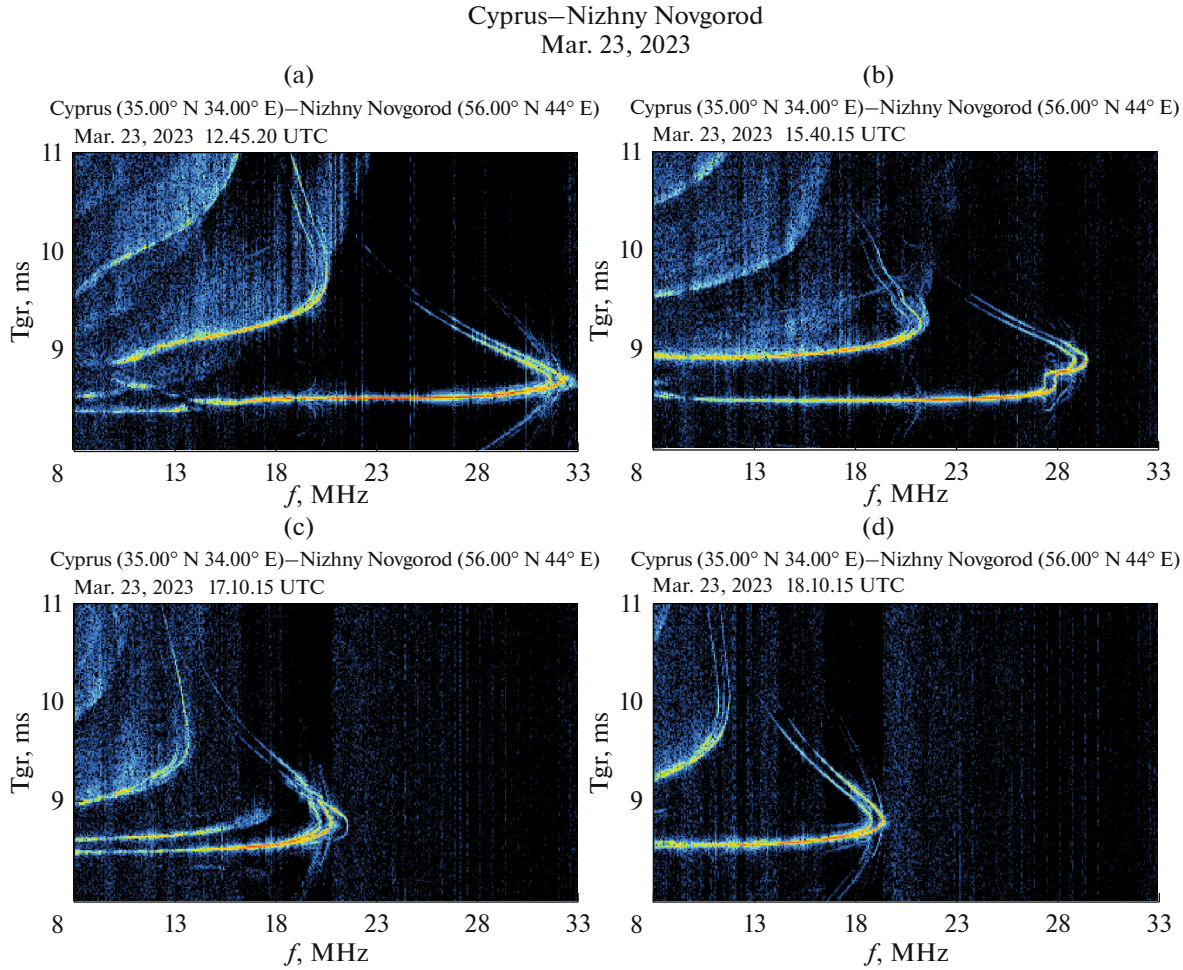

Fig. 8. Distance–frequency characteristics of the chirp signal on the Cyprus–Nizhny Novgorod sounding route on March 23, 2023 ((a) 12.45, (b) 15.40, (c) 17.10, (d) 18.10 UT).

osphere in the reflection region. Comparing the response of the ionosphere to geomagnetic disturbances on February 26–27 and March 23, 2023, it should be noted that the former were much stronger.

Comparing Figs. 2a–2c and 3a–3c, one can note that variations in the critical frequencies of the ionosphere according to data from stations located close to the same longitude are very different. They manifest themselves most weakly for the low-latitude ionosphere and strongly (up to ±3 MHz) for the high-latitude ionosphere. It was not possible to identify the source of the disturbance on March 26–31, 2023, for the Warsaw station (highlighted in red in Fig. 3b). In our opinion, this is the result of incorrect determination of the critical frequency when using computer processing of ionospheric data.

CONCLUSIONS

As a result of studies of the degree of ionospheric disturbances depending on short-term variations in solar activity (registration of coronal mass ejections and high-speed solar wind flows) based on the results of vertical and oblique sounding of the ionosphere in February and March 2023 and the use of a new ionospheric index, the presence of a pattern in the influence of a CME was confirmed on ionospheric parameters: there is a continuous decrease in values of Δf_0F_2 after the onset of a CME (loop type), whereas no significant changes are observed after the detection of other types of CMEs. The possible role of HSSs and energetic protons in the occurrence of ionospheric disturbances is noted.

Ionograms of the Vasilsursk station for vertical sounding of the ionosphere are presented, where strong absorption of the reflected signal was noted during a geomagnetic storm in February 2023. Distortions in the shape were observed in the remote-frequency characteristics of the Cyprus–Nizhny Novgorod route during geomagnetic disturbances in February–March 2023 of the *F*-layer of the ionosphere, there was a regular appearance of *z*-shaped

wave disturbances propagating to the region of lower altitudes.

FUNDING

The work was carried out within the framework of the basic part of a state order of the Ministry of Science and Higher Education of the Russian Federation, project no. FSWR-2023-0038.

CONFLICT OF INTEREST

The authors of this work declare that they have no conflicts of interest.

REFERENCES

1. Kurkin, V.I., Polekh, N.M., and Zolotukhina, N.A., Effect of weak magnetic storms on the propagation of HF radio waves, *Geomagn. Aeron. (Engl. Transl.),* 2022, vol. 62, pp. 104–115. https://doi.org/10.1134/S0016793222020116
2. Fabrizio, G.A., *High Frequency over the Horizon Radar: Fundamental Principles, Signal Processing and Practical Applications,* New York: McGraw-Hill Education, 2013.
3. Uryadov, V.P., Vybornov, F.I., Pershin, A.V., Uryadov, V.P., Vybornov, F.I., and Pershin, A.V., Variations of the frequency range of HF signals on the subauroral path during magnetic-ionospheric disturbances in October 2016, *Radiophys. Quantum Electron.,* 2021, vol. 64, no. 2, pp. 77–87. https://doi.org/10.1007/s11141-021-10113-8
4. Dem'yanov, V.V. and Yasyukevich, Yu.V., *Mekhanizmy vozdeistviya neregulyarnykh geofizicheskikh faktorov na funktsionirovanie sputnikovykh radionavigatsionnykh system* (Mechanisms of Influence of Irregular Geophysical Factors on the Functioning of Satellite Radio Navigation Systems), Irkutsk: Irkutsk. Gos. Univ., 2014.
5. Afraimovich, E.L., Gavrilyuk, N.S., Demyanov, V.V., et al., Malfunction of satellite navigation systems GPS and GLONASS caused by powerful radio emission of the Sun during solar flares on December 6 and 13, 2006, and October 28, 2003, *Cosmic Res.,* 2009, vol. 47, no. 2, pp. 146–157.
6. Zakharov, V.I., Chernyshov, A.A., Miloch, W., et al., Influence of the ionosphere on the parameters of the GPS navigation signals during a geomagnetic substorm, *Geomagn. Aeron. (Engl. Transl.),* 2020, vol. 60, no. 6, pp. 754–767. https://doi.org/10.1134/S0016793220060158
7. Zherebtsov, G.A., Shi Jiankui, Perevalova, N.P., et al., *Ionosfernye vozmushcheniya v Vostochno-Aziatskom regione* (Ionospheric Disturbances in the East Asian Region), Moscow: GEOS, 2021. https://doi.org/10.34756/GOES.2021.16.37867
8. Balan, N., Alleyne, H., Walker, S., et al., Magnetosphere-ionosphere coupling during the CME events of 07–12 November 2004, *J. Atmos. Sol.-Terr. Phys.,* 2008, vol. 70, no. 17, pp. 2101–2111.
9. Berényi, K.A., Barta, V., and Kis, A., Midlatitude ionospheric F2-layer response to eruptive solar events caused geomagnetic disturbances over Hungary during the maximum of the solar cycle 24: A case study, *Adv. Space Res.,* 2018, vol. 61, no. 5, pp. 1230–1243.
10. Burns, A.G., Solomon, S.C., Wang, W., et al., The ionospheric and thermospheric response to CMEs: Challenges and successes, *J. Atmos. Sol.-Terr. Phys.,* 2007, vol. 69, pp. 77–85. https://doi.org/10.1016/j.asr.2017.12.021
11. Qiu, N., Chen, Y.H., Wang, W.B., et al., Statistical analysis of the ionosphere response to the CIR and CME in mid-latitude regions, *Chin. J. Geophys., Chin. Ed.,* 2015, vol. 58, no. 7, pp. 2250–2262.
12. Rubtsov, A.V., Maletskii, B.M., Danilchuk, E.I., et al., Ionospheric disturbances over Eastern Siberia during April 12–15, 2016 geomagnetic storms, *Sol.-Terr. Phys.,* 2020, vol. 6, no. 1, pp. 60–68.
13. Sheiner, O.A., Fridman, V.M., Krupenya, N.D., et al., Effect of solar activity on the Earth's environment, *Proc. Second Solar Cycle and Space Weather Euroconference, ESA SP-477, Vico Equense, Italy, September 24–29, 2001,* Huguette Sawaya-Lacoste, Ed., 2002, pp. 479–481.
14. Vybornov, F.I. and Sheiner, O.A., Coronal mass ejections and high-speed solar wind streams effect on HF ionospheric communication channel, *J. Phys.: Conf. Ser.,* 2021, vol. 2131, no. 5, p. 052096. https://doi.org/10.1088/1742-6596/2131/5/052096
15. Uryadov, V.P., Vertogradov, G.G., and Vybornov, F.I., Passive over-the-horizon HF radiolocation using chirp ionosondes of various configurations for detecting and positioning ionospheric irregularities, *Naukoemkie Tekhnol.,* 2022, vol. 23, no. 5, pp. 25–33. https://doi.org/10.18127/j19998465-202205-04
16. Sheiner, O., Rakhlin, A., Fridman, V., et al., New ionospheric index for space weather services, *Adv. Space Res.,* 2020, vol. 66, no. 6, pp. 1415–1426. https://doi.org/10.1016/j.asr.2020.05.022